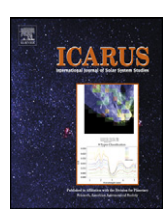


#### Contents lists available at ScienceDirect

## **Icarus**

www.elsevier.com/locate/icarus



## A survey of Karin cluster asteroids with the Spitzer Space Telescope

Alan W. Harris a,\*, Michael Mueller a,1, Carey M. Lisse b, Andrew F. Cheng b

- <sup>a</sup> DLR Institute of Planetary Research, Rutherfordstrasse 2, 12489 Berlin, Germany
- b Planetary Exploration Group, Space Department, Johns Hopkins University Applied Physics Laboratory, 11100 Johns Hopkins Rd, Laurel, MD 20723, USA

#### ARTICLE INFO

Article history:
Received 6 August 2008
Revised 25 September 2008
Accepted 26 September 2008
Available online 9 October 2008

Keywords: Asteroids Infrared observations Photometry Spectrophotometry

#### ABSTRACT

The Karin cluster is one of the youngest known families of main-belt asteroids, dating back to a collisional event only  $5.8 \pm 0.2$  Myr ago. Using the Spitzer Space Telescope we have photometrically sampled the thermal continua (3.5-22 µm) of 17 Karin cluster asteroids of different sizes, down to the smallest members discovered so far, in order to make the first direct measurements of their sizes and albedos and study the physical properties of their surfaces. Our targets are also amongst the smallest mainbelt asteroids observed to date in the mid-infrared. The derived diameters range from 17.3 km for 832 Karin to 1.5 km for 75176, with typical uncertainties of 10%. The mean albedo is  $p_v = 0.215 \pm 0.015$ , compared to  $0.20 \pm 0.07$  for 832 Karin itself (for  $H = 11.2 \pm 0.3$ ), consistent with the view that the Karin asteroids are closely related physically as well as dynamically. The albedo distribution (0.12  $\leq p_{\rm v} \leq$  0.32) is consistent with the range associated with S-type asteroids but the variation from one object to another appears to be significant. Contrary to the case for near-Earth asteroids, our data show no evidence of an albedo dependence on size. However, the mean albedo is lower than expected for young, fresh "S-type" surfaces, suggesting that space weathering can darken main-belt asteroid surfaces on very short timescales. Our data are also suggestive of a connection between surface roughness and albedo, which may reflect rejuvenation of weathered surfaces by impact gardening. While the available data allow only estimates of lower limits for thermal inertia, we find no evidence for the relatively high values of thermal inertia reported for some similarly sized near-Earth asteroids. Our results constitute the first observational confirmation of the legitimacy of assumptions made in recent modeling of the formation of the Karin cluster via a single catastrophic collision  $5.8 \pm 0.2$  Myr ago.

© 2008 Elsevier Inc. All rights reserved.

## 1. Introduction

The Karin cluster, named after its largest member, (832) Karin, is believed to have been formed  $5.8\pm0.2$  Myr ago in a catastrophic collision between two asteroids in the main belt (Nesvorný et al., 2002). This cluster is of great interest owing to the possibility that the physical properties of its members may preserve unique information about asteroid fragmentation as well as surface processes on small asteroids, which include regolith formation and modification of albedo and spectral properties by space weathering.

The Karin cluster can be identified in so-called proper element space (the proper orbital elements are approximate constants of the motion after considering perturbations from the planets) as an unusually tight grouping of objects, even when compared with the groupings that define the classical, well-known asteroid families, which are believed typically to be much older (at least hundreds of millions of years) and to have dispersed dynamically since for-

mation. The Karin cluster is found very close to the center of the Koronis family of which it is a sub-family; so detailed orbital integrations are required to distinguish Karin cluster members from background objects in the Koronis family (Nesvorný and Bottke, 2004). The extremely young reported age of the Karin cluster provides a unique opportunity to study the fragmentation of asteroids. Because of the short collisional lifetimes of small asteroids in the main belt, the young cluster age minimizes further fragmentation after the original event and limits the orbital dispersal of cluster members. Studies of the fragmentation size distribution are important because the effects of collisions shape the total asteroid size distribution (Davis et al., 2002). Collisions cause the destruction and erosion of asteroids as well as the injection of new bodies. Recent modeling (e.g., Cheng, 2004) suggests that features in the overall main-belt asteroid (MBA) size distribution, which is not a simple power law, reflect size-dependent fragmentation physics and internal structure of asteroids, but our understanding of asteroid collisional evolution is highly uncertain and incomplete. There is strong evidence that the observed infrared excesses observed in the spectra of some main-sequence stars are due to dust created by stochastic collisional fragmentation of large (>10 km) asteroids (e.g., Lisse et al., 2007). The understanding of asteroid collisions

<sup>\*</sup> Corresponding author. Fax: +49 30 67055 303.

E-mail address: alan.harris@dlr.de (A.W. Harris).

 $<sup>^{1}</sup>$  Current address: University of Arizona, Steward Observatory, 933 N Cherry Ave, Tucson, AZ 85721, USA.

 Table 1

 Observing parameters, observing geometry, and lightcurve parameters.

Asteroid & instrument		Date/time (UT)	Int. time per pixel (s)	r (AU)	d (AU)	α°	Н	Lc. amp. (mag)	Period (h)
40700	PUI	2006-01-14/12:33	5*6	3.0527	2.7376	19.1	40.0	0.00	<b>7</b> 00
10783	IRAC	2005-10-21/10:04	9*12	2.8230	2.2297	19.1	13.9	0.26	7.33
44700	PUI	2005-11-16/16:46	5*6	2.8058	2.5498	21.2	40.7	0.40	40.00
11728	IRAC	2005-09-23/12:01	9*30	2.9060	2.7848	20.6	13.7	0.19	12.92
	PUI	2006-03-15/21:17	5*6	2.9125	2.5769	19.9	44.0	0.07	6.70
16706	IRAC	2005-12-22/17:33	12*100	2.6797	2.1065	20.2	14.9	0.07	6.72
	PUI	2005-12-18/13:10	5*14	2.6806	2.0580	19.5			
28271	IRAC	2005-08-24/04:40	16*30	2.9784	2.4608	18.8	14.3	0.06-0.17	5.64
	PUI	2005-09-14/10:12	5*14	2.9777	2.7401	20.1			
33143	IRAC	2005-08-25/06:55	12*100	2.8851	2.2929	18.7	14.6	(>0.3)	
	PUI	2005-12-21/20:48	5*14	2.8768	2.2534	18.0			
34312	IRAC	2005-11-23/18:54	16*30	2.7682	2.1710	19.3	14.9	(<0.1)	
	PUI	2005-11-20/01:34	5*14	2.7667	2.1260	18.7			
40921	IRAC	2005-11-26/00:11	12*100	3.0397	2.8645	19.5	14.8	0.35	6.74
	PUI	2005-12-11/00:42	5*14	3.0434	2.6615	19.0			
41307	IRAC	2005-12-09/18:52	36*100	3.0518	3.0056	19.2	15.7	(<0.1)	
	PUI	2005-12-10/23:22	9*30	3.0519	2.9892	19.3			
43032	IRAC	2005-12-24/23:42	12*30	3.0419	2.8447	19.4	14.6	0.6	32.89
	PUI	2005-12-19/11:46	5*6	3.0424	2.9216	19.4			
55124	IRAC	2006-07-11/18:23	16*100	2.7614	2.5939	21.7	15.4	(0.25)	
	PUI	2006-07-31/08:09	5*30	2.7491	2.3287	21.2			
55434	IRAC	2005-10-23/16:46	16*100	2.9089	2.2708	17.9	15.6	(0.4)	
	PUI	2005-11-23/02:26	9*30	2.9018	2.6561	20.5			
71003	IRAC	2006-02-13/14:22	16*100	3.0388	2.4874	17.5	15.2	(0.4)	
	PUI	2006-01-14/10:06	5*30	3.0256	2.8877	19.4			
75176	IRAC	2006-06-03/23:37	36*100	3.0242	2.6635	19.2	16.5	(<0.2)	
	PUI	2006-06-24/23:04	9*30	3.0164	2.9446	19.6			
76019	IRAC	2006-05-01/00:01	36*100	2.8899	2.2867	18.0	16.1	(>0.4)	
	PUI	2007-07-26/20:28	9*30	2.9076	2.5129	20.1		, ,	
76686	IRAC	2006-06-04/13:54	16*100	2.9104	2.4748	19.6	15.2	(>0.25)	
	PUI	2005-08-15/17:33	5*30	3.0578	2.9751	19.5		, , ,	
93690	IRAC	2006-02-07/00:01	36*100	2.7612	2.1316	18.5	15.6	≥0.2	
	PUI	2005-09-12/11:59	9*30	2.7779	2.5643	21.7		y	

Note. r = heliocentric distance; d = distance from Spitzer; Lc. amp. = lightcurve amplitude. IRAC channels 1 + 3 and channels 2 + 4 exposures are separated in time by typically 20 min; the times given are the approximate mean start times of the IRAC exposures in each case. The IRS PUI 16 and 22  $\mu$ m exposures were executed back-to-back, and are between 30 s and 5 min each; the times given are the approximate mean start times of the 16 and 22  $\mu$ m exposures in each case. Integration times are given as number of on-target frames multiplied by the integration time per frame. See Table 2 for adopted H values. Lightcurve parameters for 11728 and 93690 are from Hahn et al. (2006), those for 832, 10783, 16706, 28271, 40921, 43032 are from Harris, A.W., Warner, B.D., Pravec, P. (Eds.), Asteroid Lightcurve Data. EAR-A-5-DDR-DERIVED-LIGHTCURVE-V9.0. NASA Planetary Data System, 2007. Lightcurve amplitudes in parentheses are estimates from D. Osip (personal communication).

and family formation is thus of importance for understanding planetary system development in general. The formation of the Karin family is one of the most recent occurrences of such an event in our Solar System. Nesvorný et al. (2006) have modeled the formation of the Karin cluster and conclude that the cluster was formed by a highly catastrophic disruption of a largely unfractured asteroid with a diameter of about 33 km. Our work enables crucial assumptions made by Nesvorný et al. regarding the albedo distribution and sizes of the Karin cluster members to be tested observationally for the first time.

### 2. Observations and data reduction

A total of 17 Karin cluster asteroids were observed using the Spitzer Space Telescope (hereafter Spitzer; Werner et al., 2004) between August 2005 and July 2007 (under Spitzer Cycle 2 General Observer Program #20158). Each target was imaged at six wavelengths, using the Infrared Array Camera, IRAC (Fazio et al., 2004) and the Infrared Spectrograph, IRS (Houck et al., 2004) in peak-up imaging (PUI) mode. IRAC provides four filter passbands (referred to as channels 1–4 in the following) with central wavelengths of 3.550, 4.493, 5.731, and 7.872 μm, respectively. IRS PUI provides two passbands centered at 15.8 and 22.3 μm. For more details the reader is referred to the instrument-specific data handbooks at http://ssc.spitzer.caltech.edu/irac/dh/ and http://ssc.spitzer.caltech.edu/irs/dh/.

IRAC was used in standard imaging mode. Channels 1 and 3 share a common field-of-view (FOV) using a beam splitter, as do channels 2 and 4. In most observations, channels 2 and 4 were on target for the first half of the total integration time, followed by channels 1 and 3 for the second half. At each position a standard dither pattern was executed. Observations of faint targets are subject to confusion with background sources, which can be mitigated against by taking advantage of the motion of our targets. Observations of four targets that were anticipated to be weak were designed to maximize the temporal baseline for each channel pair by having the two FOVs "take turns" on the target (see the discussion of IRAC observing strategy by Mueller, 2007): with integrations in channels 2+4 on target denoted as "A," and those in channels 1+3 on target denoted as "B," the observing patterns were ABAB for 55124 and 76686: and ABABABAB for 75176 and 76019.

Since only one Spitzer instrument is powered on at any time, the observations with the two instruments were performed at different epochs, days or weeks apart, introducing systematic uncertainties due to rotational variation of the integrated surface albedos and projected cross-sectional areas. For all observations, the respective FOV was dithered five or more times around the nominal target position using standard Spitzer dither patterns with step sizes of a few tens of arc seconds. The targets remained on chip at all dither positions. See Table 1 for a list of the target asteroids, observation times, and relevant parameters. Table 2 lists absolute magnitudes (*H* values) for the targets and those adopted for this study.

## Download English Version:

# https://daneshyari.com/en/article/1774840

Download Persian Version:

https://daneshyari.com/article/1774840

<u>Daneshyari.com</u>